Microchimica Acta
https://doi.org/10.1007/s00604-018-2698-5

ORIGINAL PAPER

Circular exponential amplification of photoinduced electron transfer using hairpin probes, G-quadruplex DNAzyme and silver nanocluster-labeled DNA for ultrasensitive fluorometric determination of pathogenic bacteria

Xueqi Leng[1] · Yu Wang[2] · Rongguo Li[3] · Su Liu[1] · Jianzhuang Yao[2] · Qianqian Pei[4] · Xuejun Cui[4] · Yuqin Tu[1] · Dan Tang[2] · Jiadong Huang[2,4]

Received: 31 October 2017 / Accepted: 20 January 2018

Abstract

The authors describe a fluorometric strategy for the detection of pathogenic bacteria with ultrasensitivity and high specificity. This strategy relies on the combination of target-modulated photoinduced electron transfer (PET) between G-quadruplex DNAzyme and DNA (labeled with silver nanoclusters) along with hairpin probe-based circular exponential amplification. The reaction system involves three hairpin probes (H1, H2 and H3). Probe H1 contains an aptamer against *S. Typhimurium* and the recognition sequence for nicking endonuclease. It is used to recognize *S. Typhimurium* and participates in polymerase-catalyzed target recycle amplification and secondary-target recycle amplification. Probe H2 contains an aptamer against hemin and is used to form the G-quadruplex DNAzyme in the presence of hemin and potassium ion. It acts as the electron acceptor and quenches the fluorescence of the labeled DNA. Fluorescence is best measured at excitation/emission wavelengths of 567/650 nm. Probe H3 contains the template sequence for the synthesis of AgNCs and the H2-annealing sequence. Both H2 and H3 are utilized to perform a strand displacement reaction and to achieve PET between G-quadruplex DNAzyme and DNA/AgNCs. To the best of our knowledge, this is the first example of a PET between G-quadruplex DNAzyme and DNA/AgNCs coupled with circular exponential amplification. The assay has an ultra-low detection limit 8 cfu·mL^{-1} of *S. Typhimurium*. The assay is rapid, accurate, inexpensive and simple. Hence, the strategy may represent a useful platform for ultrasensitive and highly specific detection of pathogenic bacteria as encountered in food analysis and clinical diagnosis.

Keywords Biosensor · Polymerase · Nicking endonuclease · Signal amplification · Strand displacement amplification · Hairpin · Gel electrophoresis · *S. Typhimurium* · Bioanalysis

Introduction

Pathogenic bacteria, a major public health concern worldwide, can cause many problems such as water pollution, hospital-acquired infections and food poisoning [1–3]. Besides pesticides, pharmaceuticals, and toxins, pathogenic bacteria are the most prominent contaminants in drinking water. It can trigger an outbreak of water-borne diseases [4]. The United States Centers for Disease Control has reported that pathogenic bacteria caused 48 million people to fall sick, 128,000 to be hospitalized, and 3000 to die each year in the United States [5]. Therefore, it is of great importance to monitor pathogenic bacteria in drinking water and the environment samples. The common method for pathogenic bacteria identification is culture and colony counting methods. Although the sensitivity of this method has been made

Electronic supplementary material The online version of this article (https://doi.org/10.1007/s00604-018-2698-5) contains supplementary material, which is available to authorized users.

✉ Su Liu
stu_lius@ujn.edu.cn

[1] College of Resources and Environment, University of Jinan, Jinan 250022, People's Republic of China

[2] College of Biological Sciences and Technology, University of Jinan, Jinan 250022, People's Republic of China

[3] Jinan Maternity and Child Care Hospital, Jinan 250022, People's Republic of China

[4] Key Laboratory of Chemical Sensing & Analysis in Universities of Shandong, College of Chemistry and Chemical Engineering, University of Jinan, Jinan 250022, People's Republic of China

Published online: 10 February 2018

great progress, it takes both time and effort for routine analysis [6]. Nowadays, enzyme-linked immunosorbent assay (ELISA) [7] and polymerase chain reaction (PCR)-based assay [8] have been developed as the effective techniques. However, these techniques suffers from the need of professional technical personal and tedious operation [9, 10]. Thereby, it's still a challenge to develop simple, rapid, inexpensive and high sensitive methods for the detection of pathogenic bacteria.

DNA-based fluorescence quantitative analysis has been recognized as an very useful technique due to their simplicity, rapidness, high sensitivity, and little proclivity to sample damage. It has been widely applied for the detection of various analytes [11–13]. One of the most used fluorescent probes is molecular beacon (MB), a hairpin-shaped nucleic acid probe labeling with a fluorescent dye and a quencher, in which the change of fluorescent signal can be modulated by the hybridization of MBs with the specific nucleic acid probes [14]. However, these fluorescent sensing strategies suffer from complicated synthesis procedure and high analysis cost. Some fluorescent metal nanoparticles, such as DNA-templated silver nanoclusters (DNA/AgNCs), have attracted considerable interest of the researchers [15–18], which possess unique photophysical properties reflected by facile synthesis, good biocompatibility, high quantum yields, tunable fluorescence colors, and excellent photostability [19]. They have been explored for effective fluorescent nanoprobes in a wide range of new application. For instance, Willner and co-workers developed a multiplexed analysis of genes using DNA/AgNCs quantum dots [20]. Dong reported a detection platform based on the assembly of grapheme oxide and DNA/AgNCs and Ye developed a label-free silver nanoclusters-assisted fluorescent sensing for sequence-specific DNA [21, 22]. Among these approaches, the fluorescence signal output is mainly dependent on fluorescence resonance energy transfer (FRET) [23, 24], and surface plasmon enhanced energy transfer (SPEET)-based photophysical mechanisms [22]. Although its widespread availability, the shortcoming of lacking of enough accuracy and efficiency for modulating the fluorescence of DNA/AgNCs needs to be further overcame. Alternatively, G-quadruplex DNAzyme can act as the electron acceptor to efficiently quench the fluorescence of certain fluorophores. It is attributed to the electron accepting ability of Fe(III)/Fe(II)-protoporphyrin IX center in the complexes. Such G-quadruplex/hemin-based electron transfer (ET) phenomenon has been developed as a novel photophysical mechanism for signal transform in the fluorescent assay strategies. For example, Wang and co-workers reported a versatile fluorescent biosensor based on photoinduced electron transfer (PET) between G-quadruplex/hemin complexes and DNA/AgNCs [25]. Yang developed a distance-dependent PET-based fluorescence light-up biosensing strategies for the detection of miRNA [26]. By the utilization of the PET mechanism, the signal switch of "OFF-ON" or "ON-OFF" can be effectively modulated by the separation or close between G-quadruplex DNAzyme and DNA/AgNCs.

The authors describe a rapid, simple and inexpensive fluorescent biosensing platform for detecting pathogenic bacteria. This assay is based on the combination of target-modulated PET between G-quadruplex DNAzyme and DNA (labeled with silver nanoclusters) along with hairpin probe-based circular exponential amplification. Considering the requirement of trace detection of pathogenic bacteria in drinking water and the environment samples, pathogenic bacteria isothermal nucleic acid amplification strategies involving of polymerase-assisted signal amplification and strand displacement amplification are integrated with target-activated PET. The reaction system includes three different hairpin probes (HAPs), polymerase, and nicking endonuclease. One of HAPs is designed to contain anti-target aptamer and the recognition sequence for nicking endonuclease. It is used for specific recognition of target and participation in polymerase-catalyzed target recycle amplification and secondary-target recycle amplification. The two other HAPs is designed to contain anti-hemin aptamer and the template sequence for AgNCs synthesis, respectively. They are utilized to execute strand displacement reaction and achieve PET between G-quadruplex DNAzyme and DNA/AgNCs. On the basis of the HAPs-based circular exponential amplification strategy, the ultrasensitivity of the method for pathogenic bacteria quantification can be achieved. Moreover, this method has the advantages of rapidness, low cost, simple operation with only one-step operation. As far as we known, this is the first report that PET between G-quadruplex DNAzyme and DNA/AgNCs coupled with HAP-based circular exponential amplification for detecting analytes. Therefore, this strategy might create an useful biosensing platform for detecting pathogenic bacteria and related food safety analysis and environmental samples inspect.

Materials and methods

Materials and reagents

All oligonucleotides were HPLC-Purified and synthesized by Sangon Biotechnology Co. Ltd. (Shanghai, China). The sequences of oligonucleotides are listed in Table S1. *Phi29* DNA polymerase (*Phi 29*) and nicking endonuclease *Nt.AlwI* (*Nt.AlwI*) were purchased from New England Biolabs (Ipswich, MA, USA). deoxyribonucleoside triphosphates (dNTPs) were purchased from Takara Biotechnology Co., Ltd. (Dalian, China). *Salmonella Typhimurium* (KCTC 1925), *E. coli* (KCTC 2571), Bacillus subtilis (KCTC 1028) and Listeria (KCTC 3569) were obtained from Institute of Microbiology Chinese Academy (Beijing, China). Peptone, beef extract powder, bacto-tryptone and bacto-yeast extract were obtained from Qingdao Biological Technology Co.

Ltd. (Qingdao, China). Agarose G-10, 10-bp DNA ladder marker and 10 × TAE buffer were from Sangon Biotech Co., Ltd. (Shanghai, China). Silver nitrate ($AgNO_3$), sodium borohydride ($NaHB_4$) and hemin were obtained from Sigma-Aldrich (St. Louis, MO). Other chemicals were of analytical grade and were used without further purification. All solutions were prepared using ultrapure water with an electric resistance >18.25 MΩ·cm, which was obtained through a Millipore Milli-Q water purification system (Billerica, MA, USA).

Apparatus

Gel electrophoresis was conducted using a DYCZ-24DN electrophoresis cell (LIUYI, Beijing, China; http://www.zg17w.cn/brand/beijingliuyi.html) and a Bio-Rad Gel imaging system (Bio-Rad, USA; http://www.bio-rad.com/). Transmission electron microscopy (TEM) measurements were made on a JEM-3010 transmission electron microscope (http://www.jeol.co.jp/). The samples for TEM characterization were prepared by adding a drop of sample solution on a carbon-coated copper grid and drying at room temperature. Fluorescence spectra were recorded using a Agilent Cary Eclipse spectrofluorometer (Agilent, USA; www.agilent.com) with excitation at 567 nm. The slit was set to be 5 nm for both the excitation and the emission.

Gel electrophoresis

The gel electrophoresis was performed at 145 V for 35 min using prepared samples (5 μL per well) on a 4% (*w*/w) agarose containing 1% (w/w) ethidium bromide in 50 mM Tris-borate running buffer (pH 7.9) containing 2 mM EDTA.. The Cyber Gold was used as an oligonucleotide dye and mixed with samples. After electrophoresis, the gel was visualized using a Bio-Rad Gel imaging system.

Transmission electron microscopy (TEM)

The samples for TEM characterization were prepared by pipetting 5 μL of the solution of samples onto a carbon-coated copper grid. After the evaporation of solvent, the grid was dried overnight. All of the images were bright-field images.

S. Typhimurium detection procedures

All samples were prepared in 6 μL Tris-HCl reaction buffer (50 mM, pH 7.4 containing 100 mM NaCl, 10 mM $MgCl_2$) for the detection of *S. Typhimurium*. The detailed procedure was as follows: H1 (3 μL, 10 μM), P (3 μL, 100 μM), 10 U phi 29, 10 U *Nt.AlwI*, 10 mM dNTPs, equal volumes (3 μL) of different concentrations of *S. Typhimurium*(or other foodborne diseases), H2 (3 μL, 100 μM), 1 μM hemin and H3 with DNA/AgNCs (20 μL, 15 μM) were mixed at 37 °C for 2 h. At last, the above mixed solution (60 μL) was mixed with 90 μL of ultrapure water and scanned using Agilent Cary Eclipse spectrofluorometer. Unless noted otherwise, all experiments for *S. Typhimurium* measurements were repeated three times.

The bacterial culture and the preparation of DNA/AgNCs are given in the Electronic Supporting Material.

Results and discussion

Principle of this biosensor for pathogenic bacteria detection

Scheme 1 illustrates the working principle of the biosensing strategy for ultrasensitive detection of pathogenic bacteria using HAP-based circular exponential amplification of PET. The HAP-based circular exponential amplification reaction includes *Nt.AlwI*-aided polymerization reaction activated by the specific binding of target and aptamer, and the strand displacement reaction designed to further amplification and signal transduction. The operate in series is at a constant temperature. To demonstrate the principle design of the strategy, *S. Typhimurium* is selected as a model analyte. The reaction system involves of three ingeniously HAP (denoted as H1, H2, and H3, respectively), one primer probe (P, denoted in blue), phi 29 polymerase, and nicking endonuclease *Nt.AlwI*. H1 is designed to contain anti-*S. Typhimurium* aptamer (denoted in red), a specific recognition sequence of *Nt.AlwI* (denoted in yellow), and a nucleic acid segment complementary to P (denoted in blue). H2 is specifically designed to contain a overhang nucleic acid segment that is anti-hemin aptamer at 3′ terminus (denoted in black), and H3 includes a overhang nucleic acid segment that is the synthesis template of DNA/AgNCs at 5′ terminus (denoted in hot pink). In our assay, DNA/AgNCs is prepared according to the previous reported methods. When target *S. Typhimurium* is introduced into the system, the specific binding of *S. Typhimurium* and aptamer induces the unfolding of H1, resulting in the hybridization of P with 3′ terminal of H1. Then P functions as a primer to initiate an extension reaction and replicates H1 with the aid of *phi 29* polymerase and dNTPs, thus the specific recognition site for *Nt.AlwI* is generated in the DNA duplex. Immediately, *Nt.AlwI* cleaves one strand of DNA, generating a new replication site for *phi 29* and releasing a single stranded-DNA (S, denoted in red). Its acts as both a secondary-target and triggers the strand displacement reaction. At the same time, the dissociated

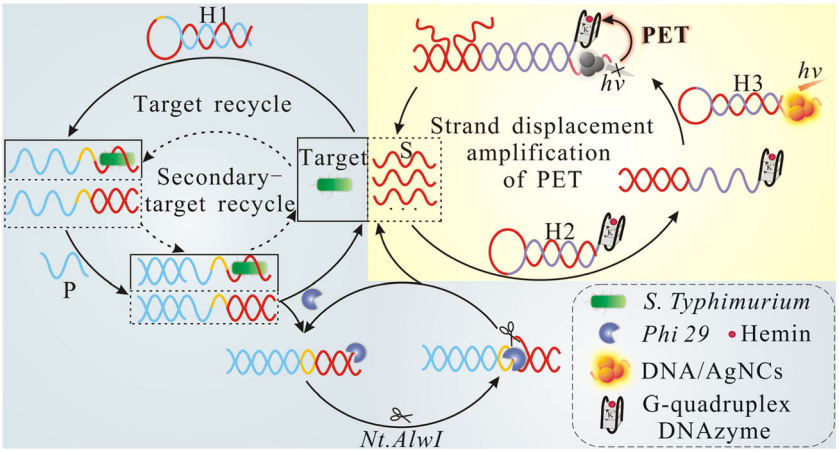

Scheme 1 Illustration of ultrasensitive fluorescent sensing of *S. Typhimurium* using HAP-based circular exponential amplification of PET

S. Typhimurium can combine to another H1, initiating new cycles of cleavage-replication reaction. Following the first stage of polymerization reaction, abundant of S is produced in the reaction system. Subsequently, S anneals with the 5′ terminus of H2 (denoted in red), resulting in the unfolding of H2 and the exposure the 3′ end of H2 (denoted in purple). The exposed 3′ terminus of H2 hybridizes with H3, triggering the strand displacement amplification (SDA) reaction, thus the H2-H3 hybrid duplex is produced and S is released. Similarly, S can bind to another H2, initiating a new cycle of SDA reaction. After the second stage of SDA reaction, a great amounts of H2-H3 duplex is generated in the system. Because G-quadruplex DNAzyme at 3′ terminus of H2 is in close proximity to DNA/AgNCs at 5′ terminus of H3, the fluorescence of DNA/AgNCs is completely quenched by G-quadruplex DNAzyme due to the PET mechanism. On the basis of the HAP-based circular exponential amplification of PET strategy, ultrasensitive and high specific detection of *S. Typhimurium* is expected to be achieved.

Validation of the PET mechanism between DNA/AgNCs and G-quadruplex DNAzyme

Three additional DNA (R, R*, and C in Table S1) was introduced to investigate the PET mechanism between G-quadruplex DNAzyme and DNA/AgNCs. R was designed to contain the nucleic acid segment complementary with R* and anti-hemin aptamer at 3′ terminus that can assembly into G-quadruplex DNAzyme in the presence of hemin. R* includes the template sequence of DNA/AgNCs at 5′ terminus and the R-annealing segment. C was designed to contain anti-hemin aptamer at 3′ terminus and the irrelevant nucleic acid segment with R*, which was used as a control DNA. The fluorescence signal before and after the hybridization of R and R* was studied to inspect the quench effect of G-quadruplex DNAzyme to DNA/AgNCs, and the results are shown in Fig. 1a. It is found that a remarkably strong fluorescent peak around 630 nm was obtained, demonstrating high quantum yield of the prepared DNA/AgNCs (curve a). However, there is very weak fluorescence signal for the R-R* hybrid duplex, implying the almost completely quenching of the fluorescence of DNA/AgNCs by G-quadruplex DNAzyme (curve b). This validated the electron transfer from DNA/AgNCs to G-quadruplex DNAzyme effectively proceeded under the condition of the close proximity of both. Additionally, when C was added into the solution containing R*, a significantly strong fluorescence signal similar with that of only R* in the solution was observed (curve c). This signifies the instant collision between the both can't induce the quenching of fluorescence of DNA/AgNCs. Furthermore, a model of the PET mechanism between the DNA/AgNCs and G-quadruplex DNAzyme was built by Molecular Operating Environment (MOE) [27]. Fig. 1b shows that the excited electrons of DNA/AgNCs are transferred to the G-quadruplex DNAzyme. By comparison of the redox state of the G-quadruplex DNAzyme and the energy levels of the DNA/AgNCs (inset of Fig. 1b), the electron transfer was proceeded according to the following mechanism:

$$\mathrm{DNA/AgNCs} + h\nu \rightarrow \mathrm{DNA/AgNCs}^{*}$$
$$\mathrm{DNA/AgNCs}^{*} + \text{G-quadruplex DNAzyme}\left(\mathrm{Fe}^{\mathrm{III}}\right) \rightarrow \mathrm{DNA/AgNCs} + \text{G-quadruplex DNAzyme}\left(\mathrm{Fe}^{\mathrm{II}}\right)$$

These results suggest that the G-quadruplex DNAzyme functions as the electron acceptor to quench the fluorescence via a PET mechanism. The Stern-Volmer plots is further used to gain insight into the quenching mechanism in Fig. S1, the related description are in Electronic Supplementary Material.

Transmission electron microscopy (TEM) measurements were employed to investigate the morphology and microstructure of the DNA/AgNCs, and the results are shown in Fig. 1c. It is observed that the average diameter of DNA/AgNCs is approximate 2.5 nm, which is consistent with the data reported

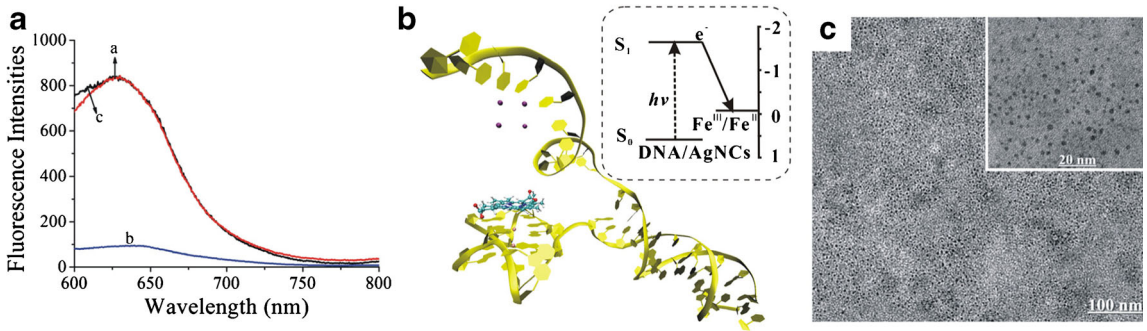

Fig. 1 **a** Fluorescence spectra responses to validate the PET mechanism. **b** The model of the PET mechanism between the DNA/AgNCs and G-quadruplex DNAzyme (inset: the energy levels of DNA/AgNCs and the redox state of G-quadruplex DNAzyme in the PET process). **c** TEM image of the prepared DNA/AgNCs

in the previous work. In addition, the prepared DNA/AgNCs is uniformly with a narrow size distribution, which is suitable for bio-analysis.

Feasibility study

To verify the feasibility of this strategy, different fluorescence response obtained upon quantifying *S. Typhimurium* in a series of control experiments were studied, and the results are depicted in Fig. 2. As shown in Fig. 2, there was a significantly strong fluorescence response for blank sample (red curve). In contrast, a negligible fluorescent signal at around 650 nm was obtained in the presence of *S. Typhimurium*, indicating the fluorescence of the vast majority of DNA/AgNCs was effectively quenched by G-quadruplex DNAzyme (magenta curve). This suggests the specific binding of target and aptamer activated HAP-based circular exponential amplification reaction, resulting in the PET between DNA/AgNCs and G-quadruplex DNAzyme due to the close proximity of both. In addition, when *Phi 29* (blue curve) or *Nt.AlwI* (green curve) was absent in the system, dramatically strong fluorescent responses similar to that of the blank sample were observed, signifying the HAP-based circular exponential amplification was initiated by *Nt.AlwI*-assited polymerization reaction. Furthermore, when non-target *E.coli* was in place of *S. Typhimurium*, a strong fluorescence was obtained, demonstrating the PET between DNA/AgNCs and G-quadruplex DNAzyme was triggered by specific binding of target and aptamer (yellow curve). On the basis of these results, it is reasonably concluded that this strategy held potential for quantitative assay of *S. Typhimurium* with high specificity.

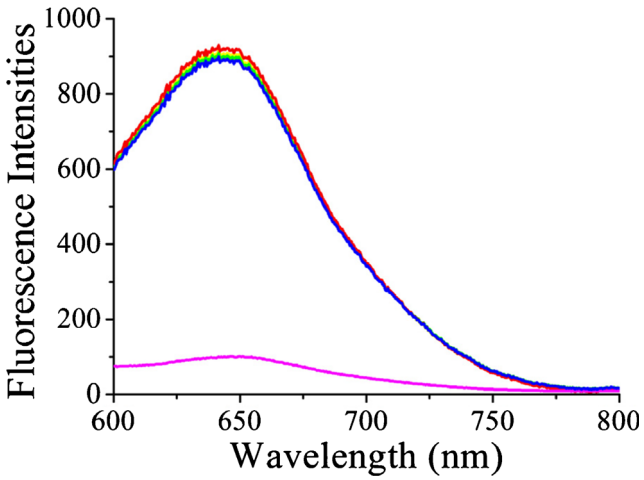

Fig. 2 Fluorescence emission spectra responses of the biosensor in the absence of *S. Typhimurium* (red curve); in the presence of 5.0×10^5 cfu·mL^{-1} *S. Typhimurium* (magenta curve); without *Phi29* DNA polymerase (blue curve); without *Nt.AlwI* (green curve); *E.coli* in place of *S. Typhimurium* (red curve). The excitation/emission wavelengths are 567 nm/650 nm

Gel electrophoresis characterization of the HAP-based circular exponential amplification

Additional evidence of the amplification strategy can be acquired through gel electrophoresis analysis. The results and related description are in Fig. S2. These results verify HAP-based circular exponential amplification is triggered by the specific binding of target and aptamer.

Optimization of experimental conditions

The following parameters were optimized: (a) concentration of hemin; (b) time of amplification reaction. Respective data and Fig. S3 are given in the Electronic Supporting Material. The following experimental conditions were found to give best results: (a) optimum concentration of hemin: 1 μM; (b) Optimal time of amplification reaction: 2 h.

Selectivity of the biosensor

To evaluate the selectivity of the biosensor for *S. Typhimurium* assay, we challenged the system with

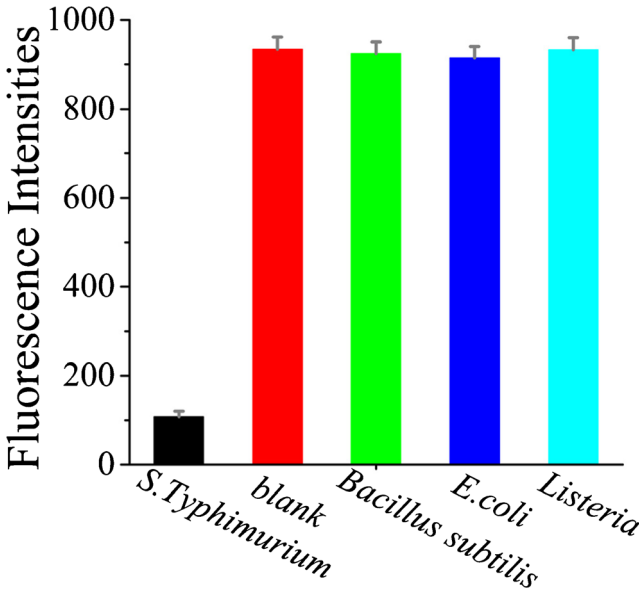

Fig. 3 Specificity evaluation of this isothermal Fluorescence assay for *S. Typhimurium* detection at excitation/emission wavelengths of 567 nm/650 nm. The concentration of *S. Typhimurium* is 5.0×10^5 cfu·mL^{-1}. The concentration of non-target bacteria is 5.0×10^7 cfu·mL^{-1}. Error bars are standard deviations across three repetitive experiments

target and several non-target pathogenic bacteria including *E.coil, Listeria, and Bacillus subtilis*. The results are shown in Fig. 3. The fluorescence intensity variation in the presence of even 100-fold excess of the non-target bacteria was all less than 4.8% compared to that of the blank sample, conforming the high specificity of the biosensor towards *S. Typhimurium* assay.

Analytical performance of the biosensor for *S. Typhimurium* detection

Under the optimal experimental conditions, the analytical performance of the biosensor were investigated towards *S. Typhimurium* at various concentrations. As seen from Fig. 4a, the fluorescence peak intensity decreased with increasing *S. Typhimurium* concentration from 0 to 5.0×10^5 cfu·mL^{-1}. A linear dependence between the peak intensity and the logarithm of *S. Typhimurium* concentration was obtained in the range from 10 cfu·mL^{-1} to 5.0×10^5 cfu·mL^{-1}, which was over 4 orders of magnitude (Fig. 4b). The linear regression equation was $F = 971.29 - 159.87 \times \log(C_{S.\ Typhimurium}$ / cfu·mL$^{-1})$ with a correlation coefficient of −0.995. The limit of detection (LOD) was calculated to be 8 cfu·mL^{-1} in terms of the rule of 3 times standard deviation over the blank response. Besides, the analytical performance of our biosensor for quantitative assay of *S. Typhimurium* was compared with that of some earlier reported methods. The results are shown in Table 1. It is found that the sensitivity of our biosensor improved at least by 2 orders of magnitude as compared to the existing methods for pathogenic bacteria assay. Moreover, this homogeneous fluorescent sensing system is implemented by only one-step operation, which offers the advantages of simplicity, rapidness, and excellent resistance to possible contaminants. As a result, our biosensor might satisfy the requirements for the profiling low abundance of *S. Typhimurium* in food and environmental samples.

Real sample analysis

To challenge the potential application of this biosensor for *S. Typhimurium* detection, we applied our fluorescent sensing in complex environment. We used this method to detect *S. Typhimurium* in milk samples. The milk from supermarket is absence of *S. Typhimurium,* so we used the quantitative assay of spiked milk samples. Different concentrations of *S. Typhimurium* (1×10, 1×10^2, 1×10^3, 1×10^4, 1×10^5 cfu·mL^{-1}) were respectively spiked into the milk samples (the dilution ratio between milk and buffer is 1:10) and the milk sample were detected by a classic plate count method and compared with the results obtained by our assay. As shown in Tab. S2., the results obtained by our method are slightly difference compared with those obtained by the plate count

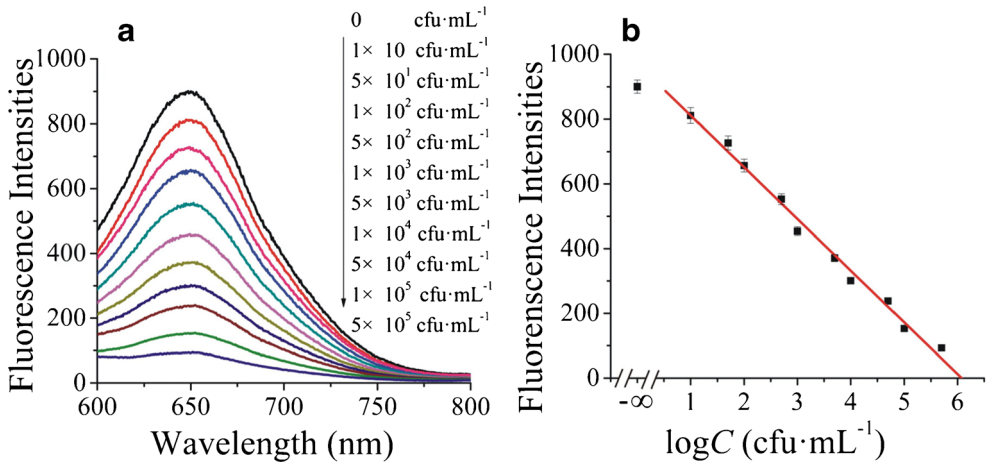

Fig. 4 **a** Fluorescence spectra responses to different concentrations of *S. Typhimurium*. **b** The calibration curve of the fluorescence intensity at excitation/emission wavelengths of 567 nm/650 nm for different *S. Typhimurium* concentrations. The error bars are standard deviations across three repetitive experiments

Table 1 Comparison of different assay methods for pathogenic bacteria determination

Detection methods	Detection range ($cfu{\cdot}mL^{-1}$)	Detection limit ($cfu{\cdot}mL^{-1}$)	The whole time of detection	Reference
Fluorescent nanospheres	1×10^5–1×10^7	1×10	5.5 h	[9]
pELISA	8×10–8×10^8	8×10^1	4.5 h	[28]
SPR	$2 \times 10^-1 \times 10^2$	2×10	10 h	[29]
Sandwich Fluorescence	1×10^3–1×10^9	2.9×10^2	3 h	[30]
Electrochemical	$6 \times 10^{2-}6 \times 10^6$	6×10^2	~4.5 h	[31]
Chemiluminescence	$5.0 \times 10^{2-}5.0 \times 10^5$	1.2×10^2	3 h	[32]
Graphene oxide-based fluorescence	1×10^3–1×10^8	1×10^2	2.75 h	[12]
Colorimetric immunoassy	$8.4 \times 10^{3-}8.4 \times 10^7$	1.7×10^3	1.5 h	[33]
Fluorescent aptasensor	1×10^2–1×10^5	3×10^2	~3 h	[34]
This work	10–5.0×10^5	8	~2 h	–

method, the discrepancies between the two methods were all smaller that 9%. The results reveal that the presence of *S. Typhimurium* in milk can be accurately detected by our fluorescent sensing, indicating it with the great applicability for real sample.

Conclusion

In summary, we have developed a simple, rapid, inexpensive fluorescence sensing strategy for pathogenic bacteria determination with ultrasensitivity and high specificity using HAP-based circular exponential amplification of PET between G-quadruplex DNAzyme and DNA/AgNCs. On the basis of the HAP-based circular exponential amplification strategy, the fluorescence sensing system can detect *S. Typhimurium* with widened detection range from 10 $cfu{\cdot}mL^{-1}$ to 5.0×10^5 $cfu{\cdot}mL^{-1}$ and a limit of detection of 8 $cfu{\cdot}mL^{-1}$. This biosensor also exhibits very high selectivity toward *S. Typhimurium* against other interfering pathogenic bacteria. Moreover, the sensing system can be implemented with only one-step homogeneous reaction. And it is simple, rapid, accurate and inexpensive. Additionally, this sensing strategy holds the potential of being extended for the detection of various aptamer binding molecules by the specific design of the probe H1. Besides, this biosensor can be used for the determination of *S. Typhimurium* in complex samples with high specificity and sensitivity. In principle, the proposed HAP-based circular exponential amplification of PET strategy belongs to "signal-off" fluorescent assays. Such "signal-off" sensing strategies suffer from limited signal capacity, in which only a maximum of 100% signal suppression can be attained under any experimental conditions. To further enhance the functionality of the sensor, "signal-on" fluorescent assay can be achieved by using DNA/AgNCs-based molecular beacon. Actually, this biosensor might create a useful and versatile platform for ultrasensitive detection of pathogenic bacteria and related food safety analysis and environmental samples inspect.

Acknowledgements This work was supported by the National Natural Science Foundation of China (31471644, 21405060), Primary Research & Development Plan of Shandong Province (2017GSF220009, 2016GSF120006) and Shandong Province Natural Science Foundation of China (ZR2016BL27).

Compliance with ethical standards The author(s) declare that they have no competing interests.

References

1. Duan N, Wu S, Dai S, Miao T, Chen J, Wang Z (2015) Simultaneous detection of pathogenic bacteria using an aptamer based biosensor and dual fluorescence resonance energy transfer from quantum dots to carbon nanoparticles. Microchim Acta 182: 917–923
2. Tokonami S, Nakadoi Y, Takahashi M, Ikemizu M, Kadoma T, Saimatsu K, Dung L, Shiigi H, Nagaoka T (2013) Label-free and selective bacteria detection using a film with transferred bacterial configuration. Anal Chem 85:4925–4929
3. Leng XQ, Wang Y, Liu S, Pei QQ, Cui XJ, Tu YQ, Liu XJ, Huang JD (2017) Enzymatic repairing amplification-based versatile signal-on fluorescence sensing platform for detecting pathogenic bacteria. Sens Actuators B: Chem 252:689–696
4. Donhauser SC, Niessner R, Seidel M (2011) Sensitive quantification of Escherichia Coli O157: H7, salmonella enterica, and campylobacter jejuni by combining stopped polymerase chain reaction with chemiluminescence flow-through DNA microarray analysis. Anal Chem 83:3153–3160
5. Scallan E, Griffin PM, Angulo FJ, Tauxe RV, Hoekstra RM (2011) Foodborne illness acquired in the United States-unspecified agents. Emerging Infect Dis 17:16–22
6. Brooks BW, Devenish J, Lutze-Wallace CL, Milnes D, Robertson RH, Berlie S (2004) Evaluation of a monoclonal antibody-based enzyme-linked immunosorbent assay for detection of

campylobacter fetus in bovine preputial washing and vaginal mucus samples. G Vet Microbiol 103:77–84
7. Pappert G, Rieger M, Niessner R, Seidel M (2010) Immunomagnetic nanoparticle-based sandwich chemiluminescence-ELISA for the enrichment and quantification of *E. coli*. Microchim Acta 168:1–8
8. Roda A, Mirasoli M, Roda B, Bonviciniv F, Colliva C (2012) Recent developments in rapid multiplexed bioanalytical methods for foodborne pathogenic bacteria detection. Microchim Acta 178: 7–28
9. Wen CY, Hu J, Zhang ZL, Tian ZQ, Ou GP, Liao YL, Li Y, Xie M, Sun ZY, Pang DW (2013) One-step sensitive detection of salmonella typhimurium by coupling magnetic capture and fluorescence identification with functional nanospheres. Anal Chem 85:1223–1230
10. Roda A, Mirasoli M, Roda B, Bonvicini F, Colliva C, Reschiglian P (2012) Recent developments in rapid multiplexed bioanalytical methods for foodborne pathogenic bacteria detection. Microchim Acta 178:7–28
11. Nakano S, Fukuda M, Tamura T, Sakaguchi R, Nakata E, Morii T (2013) Simultaneous detection of ATP and GTP by covalently linked fluorescent ribonucleopeptide sensors. J Am Chem Soc 135:3465–3473
12. Duan YF, Ning Y, Song Y, Deng L (2014) Fluorescent aptasensor for the determination of salmonella typhimurium based on a graphene oxide platform. Microchim Acta 181:647–653
13. Zhang Y, Tang L, Yang F, Sun Z, Zhang GJ (2015) Highly sensitive DNA-based fluorometric mercury(II) bioassay based on graphene oxide and exonuclease III-assisted signal amplification. Microchim Acta 182:1535–1541
14. Tyagi S, Kramer F (1996) Molecular beacons: probes that fluoresce upon hybridization. Nat Biotechnol 14:303–308
15. Katz E, Willner I (2004) Integrated nanoparticle–biomolecule hybrid systems: synthesis, properties, and applications. Angew Chem Int Ed 43:6042–6108
16. Feng C, Tu J, Liang C, Yang B, Chen C, Chen X (2016) Fluorescent drug screening based on aggregation of DNA-templated silver nanoclusters, and its application to iridium (III) derived anticancer drugs. Microchim Acta 183:1571–1577
17. Bruchez M, Moronne M, Gin P, Weiss S, Alivisatos AP (1998) Semiconductor nanocrystals as fluorescent biological labels. Science 281:2013–2016
18. Medintz IL, Uyeda HT, Goldman ER, Mattoussi H (2005) Quantum dot bioconjugates for imaging, labelling and sensing. Nat Mater 4:435
19. Petty JT, Story SP, Juarez S, Votto SS, Herbst AG, Degtyareva NN, Sengupta B (2011) Optical sensing by transforming chromophoric silver clusters in DNA nanoreactors. Anal Chem 84:356–364
20. Enkin N, Sharon E, Golub E, Willner I (2014) Ag nanocluster/DNA hybrids: functional modules for the detection of nitroaromatic and RDX explosives. Nano Lett 14:4918–4922
21. Fan D, Zhu J, Liu Y, Wang E, Dong S (2016) Label-free and enzyme-free platform for the construction of advanced DNA logic devices based on the assembly of graphene oxide and DNA-templated AgNCs. Nano 8:3834–3840
22. Ma JL, Yin BC, Le HN, Ye BC (2015) Label-free detection of sequence-specific DNA based on fluorescent silver nanoclusters-assisted surface plasmon-enhanced energy transfer. ACS Appl Mater Interfaces 7:12856–12863
23. Enkin N, Wang F, Sharon E, Albada HB, Willner I (2014) Multiplexed analysis of genes using nucleic acid-stabilized silver-nanocluster quantum dots. ACS Nano 8:11666–11673
24. Wu M, Xu X, Wang J, Li L (2015) Fluorescence resonance energy transfer in a binary organic nanoparticle system and its application. ACS Appl Mater Interfaces 7:8243–8250
25. Zhang L, Zhu J, Guo S, Li T, Li J, Wang E (2013) Photoinduced electron transfer of DNA/ag nanoclusters modulated by G-quadruplex/hemin complex for the construction of versatile biosensors. J Am Chem Soc 135:2403–2406
26. Lu S, Wang S, Zhao J, Sun J, Yang X (2017) Fluorescence light-up biosensor for MicroRNA based on the distance-dependent Photoinduced electron transfer. Anal Chem 89:8429–8436
27. *Molecular Operating Environment (MOE)*, 2013.08; Chemical Computing Group ULC, 1010 Sherbooke St. West, Suite #910, Montreal, QC, Canada, H3A 2R7, 2017
28. Chen R, Huang X, Xu H, Xiong Y, Li Y (2015) Plasmonic enzyme-linked immunosorbent assay using nanospherical brushes as a catalase container for colorimetric detection of ultralow concentrations of listeria monocytogenes. ACS Appl Mater Interfaces 7:28632–28639
29. Bulard E, Bouchet-Spinelli A, Chaud P, Roget A, Calemczuk R, Fort S, Livache T (2015) Carbohydrates as new probes for the identification of closely related Escherichia coli strains using surface plasmon resonance imaging. Anal Chem 87:1804–1811
30. Kong W, Xiong J, Yue H, Fu Z (2015) Sandwich fluorimetric method for specific detection of Staphylococcus Aureus based on antibiotic-affinity strategy. Anal Chem 87:9864–9868
31. Wang X, Zhu P, Pi F, Jiang H, Shao J, Zhang Y, Sun X (2016) A sensitive and simple macrophage-based electrochemical biosensor for evaluating lipopolysaccharide cytotoxicity of pathogenic bacteria. Biosens Bioelectron 81:349–357
32. Li Z, Yang H, Sun L, Qi H, Gao Q, Zhang C (2015) Electrogenerated chemiluminescence biosensors for the detection of pathogenic bacteria using antimicrobial peptides as capture/signal probes. Sens. Actuators B: Chem. 210:468–474
33. Zhu H, Zhao G, Wang SQ, Dou W (2017) Photometric sandwich immunoassay for salmonella pullorum and Salmonella Gallinarum using horseradish peroxidase and magnetic silica nanoparticles. Microchim Acta 184:1873–1880
34. Liu K, Yan X, Mao B, Wang S, Deng L (2016) Aptamer-based detection of Salmonella enteritidis using double signal amplification by Klenow fragment and dual fluorescence. Microchim Acta 183:643–649